A Null Lesion in the Rhodopin 3,4-Desaturase of *Rhodospirillum rubrum* Unmasks a Cryptic Branch of the Carotenoid Biosynthetic Pathway†

Mika Komori,‡ Robin Ghosh,§,|| Shinichi Takaichi,⊥ Ying Hu,‡ Tadashi Mizoguchi,‡ Yasushi Koyama,‡ and Michitaka Kuki*,#

Faculty of Science, Kwansei Gakuin University, Uegahara, Nishinomiya 662-8501, Japan, Laboratory of Bioenergetics, University of Geneva, Chemin des Embrouchis 10, CH-1254 Jussy-Lullier/GE, Switzerland, Biological Laboratory, Nippon Medical School, Kosugi-cho 2, Nakahara-ku, Kawasaki 221-0063, Japan, and Department of Applied Chemistry, Kobe City College of Technology, Gakuen-Higashimachi, Nishi-ku, Kobe 651-2194, Japan

Received December 16, 1997; Revised Manuscript Received March 19, 1998

ABSTRACT: The carotenoids accumulated by a mutant *Rhodospirillum rubrum* ST4, containing a single Tn5 lesion in the pathway for carotenoid biosynthesis, were analyzed by HPLC, ^{1}H NMR spectroscopy, and field desorption mass spectrometry. The main carotenoid was identified as 3,4,3′,4′-tetrahydrospirilloxanthin, and the four minor carotenoids were identified as rhodopin, 3,4-dihydroanhydrorhodovibrin, 3′,4′-dihydrorhodovibrin, and 1,1′-dihydroxylycopene. The C-3,4 and C-3′,4′ bonds of all 5 carotenoids are saturated, and they have 11 conjugated double bonds. With the exception of rhodopin, which is a normal intermediate of the wild-type pathway, all of the carotenoids are not naturally occurring. The Tn5 lesion was assigned to rhodopin 3,4-desaturase which is proposed to catalyze dehydrogenation at both ends of the symmetrical spirilloxanthin derivative. An unexpected finding was that the enzymes following rhodopin 3,4-desaturase are still able to end-modify the 3,4-, and 3′,4′-saturated precursors and that the order of methylation and hydroxylation is not obligatory. It is proposed that the observed nonnatural carotenoids can be explained by the inclusion of a cryptic branch, unmasked by the absence of rhodopin 3,4-desaturase, in the established linear pathway for spirilloxanthin biosynthesis. This is the first example of latent branching of the carotenoid biosynthesis pathway exhibited by a carotenoid mutant of a phototrophic bacterium.

Carotenoids are widely occurring in nature and fulfill a variety of functions including light-harvesting and energy transfer in photosynthesis as well as for photoprotection, coloration, and as pigments of the visual signal transduction process (*1*). The initial steps of carotenoid biosynthesis appear to be highly conserved throughout plant, animal (although in animals some of the intermediate steps are absent), and microbial kingdoms (*2*−*10*), providing a striking example of the metabolic flexibility utilized to synthesize long polyunsaturated hydrocarbon chains from repeating isoprene units.

In the purple bacteria, *Rhodobacter capsulatus* and *Rhodobacter sphaeroides*, the enzymes for the biosynthesis of the major C_{40} carotenoids spheroidene and hydroxyspheroidene have now been well-characterized at the gene level. Thus, the 10 steps of carotenoid biosynthesis starting from farnesyl pyrophosphate and leading to spheroidenone and hydroxyspheroidenone are catalyzed by enzymes encoded by 7 genes, *crtA*,[1] *crtB*, *crtC*, *crtD*, *crtE*, *crtF*, and *crtI*, which are found in 4 adjacent operons of the 46 kb photosynthetic gene cluster (*psg* cluster) in these organisms. A full description of the gene products and their assigned enzyme activities has been given elsewhere (*6*, *11*−*13*).

The assignment of the biosynthetic steps generating carotenoid precursors to the gene products revealed that in several cases, a single enzyme catalyzes several metabolic reactions. Most striking is that phytoene desaturase (encoded by the gene *crtI*) mediates 3−4 sequential desaturation steps starting from phytoene and leading either to neurosporene [in *Rb. capsulatus* (*2*−*4*, *14*, *15*) and *Rb. sphaeroides* (*12*, *16*, *17*)] or to lycopene [in *Erwinia uredovora* (*18*), *Erwinia herbicola* (*19*), and *Rhodospirillum rubrum* (M. Wiggli and R. Ghosh, unpublished data)].

In *Rb. sphaeroides* and *Rb. capsulatus*, the 1- and 1′-hydroxylation steps of neurosporene and spheroidene, leading to the products hydroxyneurosporene and hydroxyspheroidene, respectively, are also catalyzed by a single hydratase, CrtC. In addition, the *crtD* gene product can catalyze the 3,4-desaturation of either hydroxyneurosporene

† R.G. was funded by the Swiss Priority Program for Biotechnology (Grants 5002-41801 and 5002-39816).

* To whom correspondence should be addressed. E-mail: kuki@kobe-kosen.ac.jp. Fax: +81-78-795-3314.

‡ Kwansei Gakuin University.

§ University of Geneva.

|| Present address: Department of Bioenergetics, Institute of Biology, University of Stuttgart, Pfaffenwaldring 57, D-70550 Stuttgart, Germany.

⊥ Nippon Medical School.

Kobe City College of Technology.

[1] Abbreviations: *crt*, carotenoid gene designation; DPA, diphenylamine; FD-MS, field desorption mode of mass spectrometry; HPLC, high-performance liquid chromatography; NMR, nuclear magnetic resonance; *psg*, photosynthetic gene cluster; Q_y, near-infrared absorption maximum of bacteriochlorophyll **a**; RC, reaction center; LH I, light-harvesting complex I.

S0006-2960(97)03094-8 CCC: $15.00
Published on Web 05/30/1998

or methoxyneurosporene, and the *O*-methyltransferase CrtF can methoxylate the 1-hydroxyl moiety of either hydroxyneurosporene (3,4-saturated) or demethylspheroidene (3,4-desaturated). Finally, under semi-aerobic conditions, the oxygenase CrtA can utilize either spheroidene (1-methoxylated, 3,4-desaturated), demethylspheroidene (1-hydroxylated, 3,4-desaturated), or hydroxyspheroidene (1-methoxylated, 1′-hydroxylated, 3,4-desaturated) to form spheroidenone, demethylspheroidenone, and hydroxyspheroidenone, respectively. The broad substrate specificities of the *crt* gene products would be expected to generate a branched biosynthetic pathway in vivo, which has been confirmed experimentally for both *Rb. capsulatus* (*3*, *15*) and *Rb. sphaeroides* (*12*).

In *R. rubrum*, the initial desaturation steps of the carotenoid biosynthetic pathway leading to the symmetrical polyunsaturated C_{40} carotenoid spirilloxanthin are also mediated by phytoene desaturase (CrtI). In this case, however, CrtI catalyzes 4 desaturation steps, leading to the intermediate, lycopene, which possesses 11 conjugated double bonds located between the 5- and 5′-positions of the carbon chain. Chemical and physicochemical analyses of the pathway in *R. rubrum* have demonstrated that the subsequent hydroxylation, dehydrogenation, and methoxylation steps are carried out sequentially with no observed branching (*20*−*22*), although a recent physicochemical study has suggested that two pathways may be involved (*23*). In early studies, however, Davies and co-workers (*22*, *24*−*26*) demonstrated that the addition of diphenylamine (DPA) to the culture medium of photoheterotrophically growing *R. rubrum* led to a large number of nonnatural carotenoid products, presumably due to nonspecific branching of the pathway. The mechanism of action of DPA has not been characterized, so the physiological significance of the DPA inhibition experiments has remained unclear until now. However, it has been shown that DPA causes an accumulation of phytoene, suggesting that the phytoene desaturase (CrtI) is one locus of inhibition.

Recently, one of us (R.G.) has begun to characterize the 46 kb *psg* cluster in *R. rubrum*, which encodes all the genes for carotenoid and bacteriochlorophyll biosynthesis, as well as the gene encoding the α- and β-polypeptides of the light-harvesting complex I (LH I) and the H-, L-, and M-polypeptides of the reaction center (RC) (*27*; R. Saegesser, R. Bachofen, and R. Ghosh, unpublished data, full details to be published elsewhere). In the course of these studies, we have isolated a brown Tn5 mutant with a single lesion in the 46 kb *psg* cluster. We show here that the disrupted gene probably encodes a 3,4-desaturase and that its absence leads to the production of nonnatural carotenoid products due to latent branching of the biosynthetic pathway. This is the first time that latent branching unmasked by the introduction of a null lesion has been found in a photosynthetic procaryote, and it suggests that the substrate specificities of the *crt* enzymes in *R. rubrum* may be broader than those for the corresponding enzymes of the related organisms *Rb. capsulatus* and *Rb. sphaeroides*.

MATERIALS AND METHODS

Growth of Bacteria and Tn5 Mutagenesis. For routine purposes, cells of *R. rubrum* were grown under anaerobic, photoheterotrophic conditions using Sistrom medium A (*28*). Tn5 mutagenesis of the wild-type *R. rubrum* S1 was performed (using the suicide vector pSUP202::Tn5) as described (*29*, *30*), and mutants were selected by their ability to grow aerobically in the presence of kanamycin. Kanamycin-resistant cells were then tested for photoheterotrophic growth. Cells to be used as starting material for carotenoid extraction were grown either photoheterotrophically using Sistrom medium A or semi-aerobically under chemoheterotrophic conditions using a modified Sistrom medium (M2SF) (*31*) which uses both succinate and fructose as carbon sources. The anaerobic, photoheterotrophic cultures were grown in sealed bottles under low light (500 W/m^2), and the semi-aerobic, chemoheterotrophic cultures were grown in the dark in a 50 L batch culture with the partial pressure of oxygen regulated to less than 1%. In both cases, the cultures were harvested in the late exponential phase by centrifugation and washed with 200 mL of 20 mM Tris-HCl, pH 8.0. The washed cell paste was then frozen in liquid nitrogen for storage.

Pigment Extraction for High-Performance Liquid Chromatography (HPLC) Analysis. Pigments were extracted 3 times from whole cells (2 g wet weight) with 10 mL of acetone/methanol (7:2, v/v), and then dried in vacuo. The extract was dissolved in 10 mL of dichloromethane/methanol (3:1, v/v) at room temperature, and a 20 μL aliquot of this solution was analyzed by HPLC. All manipulations were performed in the dark. The HPLC analysis was performed by using a home-packed Spherisorb ODS2 5 μm (Waters) column (4.6 mm i.d. × 250 mm) and gradient elution with ethyl acetate (solution A) and acetonitrile/water (9:1) containing 0.1% triethylamine (solution B). The applied gradient was as follows: 0−15 min, 23% A; 15−30 min, 23−70% A; 30−40 min, 70−100% A; 40−45 min, 100% A (*32*). The flow rate was 1 mL/min, and the detection wavelength was 470 nm. Electronic absorption spectra (300−800 nm) in the eluent were recorded with a Waters 996 photodiode-array detector.

Purification of Carotenoids for Nuclear Magnetic Resonance (NMR) and Field Desorption Mode of Mass Spectrometry (FD-MS) Measurements. Initially, the bulk of the bacteriochlorophyll and water was removed from cell paste (80 g wet weight) by a single extraction with approximately 200 mL of methanol. Extraction was performed by stirring the methanol/cell paste suspension with a glass rod. Dehydrated pellets were extracted 3 times with approximately 200 mL of acetone as above. To the pooled acetone extract (1 volume) were added *n*-hexane (1 volume) and water (1 volume) to transfer the pigments to the *n*-hexane layer. The *n*-hexane fraction was dried in vacuo and dissolved in approximately 600 mL of *n*-hexane. Each carotenoid was isolated and purified by alumina [Merck, activity II−III; deactivated with 5% (v/w) of water] column chromatography developed with a stepwise gradient of 3−30% diethyl ether/*n*-hexane. (This chromatographic step was performed twice.) Carotenoid fractions were dried and dissolved in benzene for storage. Further, each carotenoid corresponding to peaks 2, 4, and 5 (Figure 1b) was crystallized as follows. Each carotenoid was dissolved in a minimum volume of benzene, and *n*-hexane was added until the solution was just clouded. Then, the mixture was left in the freezer (−20 °C).

NMR Measurements. The 400 MHz 1D and 2D COSY, long-range COSY, and ROESY ^{1}H NMR spectra were

recorded at 8 °C in benzene-d_6 (CEA 99.6%) by a JEOL JNM-A400FT NMR spectrometer. The peak of benzene was used as reference (7.16 ppm). The details were described elsewhere (*33*).

Molecular Masses. Molecular masses of the carotenoids and their trimethylsilyl derivatives (to determine the number of hydroxyl group) were analyzed with FD-MS as described elsewhere (*34*).

RESULTS

Phenotypic Characterization of the Mutant R. rubrum ST4. Following a round of random Tn5 mutagenesis, a brown kan^R mutant of *R. rubrum* (designated *R. rubrum* ST4) was obtained. This mutant grew well under anaerobic, photoheterotrophic conditions at both high and low light intensities as well as under aerobic and semi-aerobic conditions. The growth kinetics and yield appear to be identical to those of the wild-type *R. rubrum* S1. Southern hybridization using the Tn5 element as a probe indicated a single lesion in the chromosome (data not shown). The mutant could be complemented with both cosmids pSC4 and pSC6, which were obtained from the pVK100-derived gene bank of *R. rubrum* S1 (R. Ghosh, unpublished data). Mapping of the cosmids allowed the *crt* lesion to be localized to the *psg* cluster of *R. rubrum.*

The absorption spectrum of whole cells of the mutant *R. rubrum* ST4 revealed that the three typical absorption maxima of the carotenoid region were shifted approximately 25 nm to the blue compared to those of spirilloxanthin in the wild type (Figure 1a). However, the near-infrared absorption maximum (Q_y) of the LH I antenna bacteriochlorophyll was still observed at 882 nm, identical to the wild-type. The transconjugants *R. rubrum* ST4 (pSC4) and *R. rubrum* ST4 (pSC6) recovered the wild-type carotenoid spectrum.

Analysis of Carotenoids. Figure 1b shows the elution profile of the pigment extract from the cells of *R. rubrum* ST4 at 470 nm (solid line) and 750 nm (broken line). Peaks 1−5 were identified as carotenoids from their absorption spectra. The other peaks at 9, 22, and 29 min were identified from their absorption spectra as bacteriochlorophyll **a**, bacteriopheophytin, and a bacteriochlorophyll derivative, respectively. Table 1 lists the compound name, the corresponding absorption maxima in the eluent, the number of conjugated double bonds present, the respective molecular masses, and the number of hydroxyl groups determined by FD-MS, as well as the carotenoid composition. Table 1 also lists those of spirilloxanthin for comparison.

The last (red) absorption maxima (0−0 transition) of carotenoids with different conjugated chains in *n*-hexane are as follows: neurosporene (9 conjugated double bonds), 468 nm; spheroidene (10 conjugated double bonds), 486 nm; lycopene (11 conjugated double bonds), 502 nm; 3,4-dihydrospirilloxanthin (12 conjugated double bonds), 515 nm; and spirilloxanthin (13 conjugated double bonds), 526 nm (*35*, *36*). For spirilloxanthin, the red shift observed after changing solvents from *n*-hexane to the eluent is only 5 nm. On the other hand, the effect of increasing a double bond in a conjugated chain causes a red shift of more than 11 nm. The number of conjugated double bonds of the carotenoids can be estimated by the position of the absorption maxima.

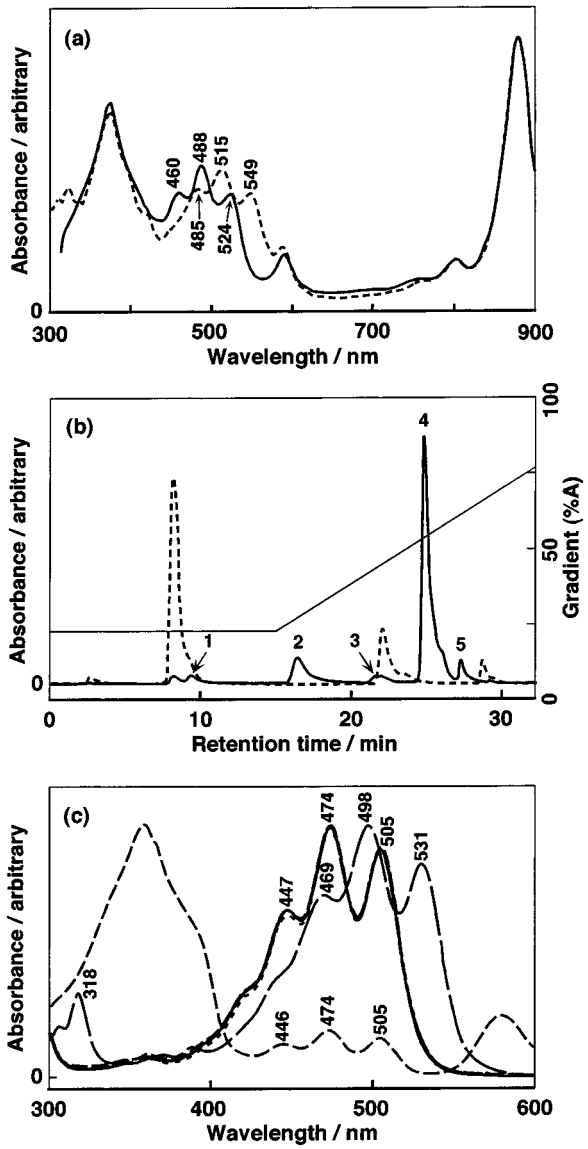

FIGURE 1: (a) Absorption spectra of the whole cells, suspended in 80% glycerol and 20% Sistrom medium A, of *R. rubrum* ST4 (—) and S1 (- - -). (b) HPLC elution profile of the extracted pigments from *R. rubrum* ST4 measured at 470 nm (—) and at 750 nm (- - -). The HPLC conditions are described under Materials and Methods. (c) Absorption spectra of the HPLC peaks shown in (b). The spectra of peaks 1 (- - -), 2 (- · -), 3 (···), 4 (—), and 5 (- ·· -) as well as spirilloxanthin (— —) are indicated. The absorption maxima corresponding to bacteriochlorophyll **a** are not indicated.

The absorption maxima of the 5 carotenoids and lycopene are almost the same (Figure 1c), indicating that the 5 carotenoids have 11 conjugated double bonds. Takaichi and Shimada (*37*) have observed that for carotenoids with linear end groups the ratios (%III/II, expressed as a percentage) of the last (red) absorption maximum (0−0 transition) to that of the middle (second) absorption maximum (0−1 transition), as measured from the minimum between the two peaks, are generally over 60%. The carotenoids isolated here all have a %III/II of >60%, thus indicating that they are acyclic.

Peaks 2, 4, and 5 (Figure 1b) were identified mainly by 1D and 2D ^{1}H NMR spectroscopy. Table 2 lists ^{1}H-^{1}H correlations detected in COSY and long-range COSY, and Table 3 lists the values of chemical shifts for all the protons. Figure 2 shows the numbering of the carbon atoms in the carotenoid backbone and the NOE correlations with arrows.

Table 1: Properties of the Carotenoids Isolated from *R. rubrum* ST4

peak no. in Figure 1b	carotenoid	λ_{max} (nm) in eluent			%III/II	no. of conjugated double bonds	molecular mass	no. of hydroxyl groups	carotenoid composition (% total found)[d]
1	1,1′-dihydroxylycopene	446	474	505		11	–	–	2.7[a]
2	3′,4′-dihydrorhodovibrin	447	474	505	76	11	586	1	11.6 (6)[b]
3	rhodopin	447	474	505	77	11	554	1	1.5 (1)[b]
4	3,4,3′,4′-tetrahydrospirilloxanthin	447	474	505	75	11	600	0	77.8 (91)[b]
5	3,4-dihydroanhydrorhodovibrin	447	474	505	74	11	568	0	5.9 (2)[b]
	lycopene[c]	447	474	505		11	–	–	0.4
	spirilloxanthin	469	498	531	64	13	596	0	–

[a] No corresponding carotenoid in wild type. [b] The value in parentheses denotes the composition of the corresponding carotenoid (see Figure 3) in the wild-type S1 (see ref *45*). [c] Present in trace amounts in *R. rubrum* ST4 (data not shown). [d] Obtained by integration of the HPLC profile.

Table 2: $^1H-^1H$ Correlations Detected in Two-Dimensional Spectra of (a) 3,4,3′,4′-Tetrahydrospirilloxanthin, (b) 3′,4′-Dihydrorhodovibrin, and (c) 3,4-Dihydroanhydrorhodovibrin

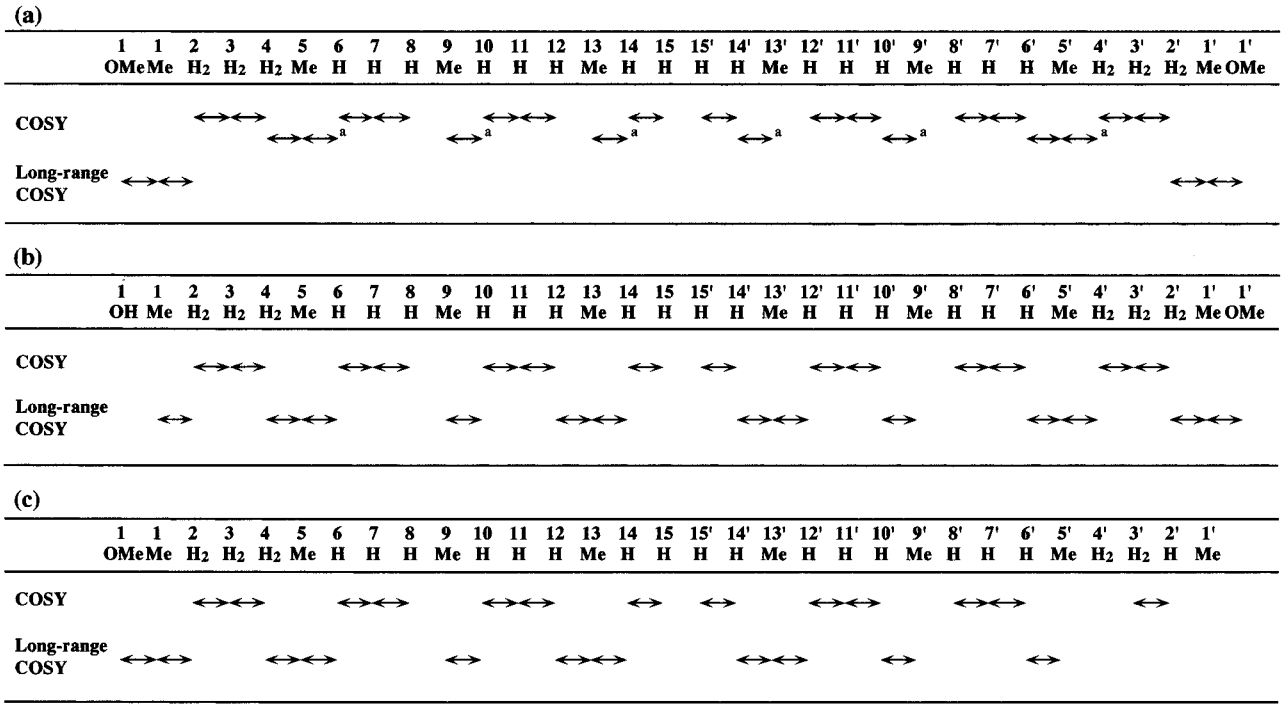

[a] These correlations are usually detected by long-range COSY. However, in this carotenoid, the correlations were detected by COSY.

Table 3: Chemical Shifts of 3,4,3′,4′-Tetrahydrospirilloxanthin, 3′,4′-Dihydrorhodovibrin, and 3,4-Dihydroanhydrorhodovibrin in Benzene-d_6 (ppm)

3,4,3′,4′-tetrahydrospirilloxanthin				3′,4′-dihydrorhodovibrin				3,4-dihydroanhydrorhodovibrin			
1OMe	3.04	6H	6.19	1OMe	0.59	6H	6.18	1OMe	3.04	6H	6.20
1′OMe		6′H		1′OMe	3.04	6′H	6.19			6′H	6.18
1Me	1.06	7H	6.71	1Me	1.03	7H	6.72	1Me	1.06	7H	6.71
1′Me		7′H		1′Me	1.06	7′H	6.71	1′Me	1.57, 1.68	7′H	6.69
5Me	1.76	8H	6.47	5Me	1.75	8H	6.49	5Me	1.76	8H	6.48
5′Me		8′H		5′Me	1.76	8′H	6.47	5′Me	1.75	8′H	6.46
9Me	1.94	10H	6.39	9Me	1.95	10H	6.39	9Me	1.94	10H	6.39
9′Me		10′H		9′Me	1.94	10′H		9′Me	1.93	10′H	6.37
13Me	1.88	11H	6.79	13Me	1.88	11H	6.79	13Me	1.88	11H	6.79
13′Me		11′H		13′Me		11′H		13′Me		11′H	
$2H_2$	1.41	12H	6.51	$2H_2$	1.32	12H	6.51	$2H_2$	1.41	12H	6.51
$2'H_2$		12′H		$2'H_2$	1.41	12′H		2′H	5.25	12′H	
$3H_2$	1.58	14H	6.36	$3H_2$	1.49	14H	6.36	$3H_2$	1.58	14H	6.36
$3'H_2$		14′H		$3'H_2$	1.58	14′H		$3'H_2$	2.19	14′H	
$4H_2$	2.09	15H	6.72	$4H_2$	2.06	15H	6.72	$4H_2$	2.09	15H	6.72
$4'H_2$		15′H		$4'H_2$	2.09	15′H		$4'H_2$	2.19	15′H	

The COSY peaks correlate proton pairs separated by three bonds (i.e., between protons of each neighboring carbon), and the long-range COSY peaks correlate proton pairs separated by four bonds (e.g., between the protons of a methyl group and an adjacent proton). Thus, both measurements allow the determination of carotenoid structure. On

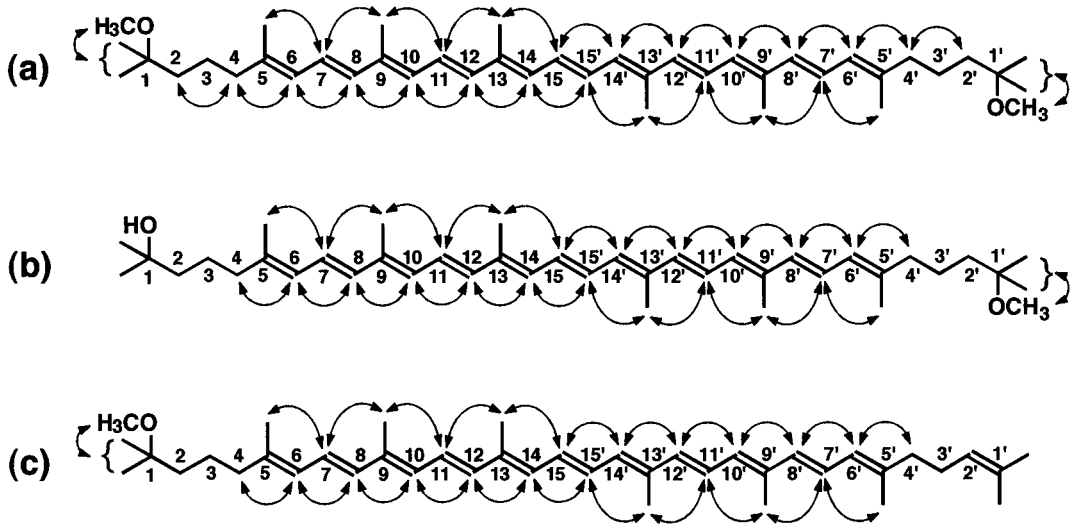

FIGURE 2: Chemical structures of the carotenoids of *R. rubrum* ST4. NOE correlations which were identified in the ROESY spectra and facilitated the configurational determinations are shown with arrows. (a) *all-trans*-3,4,3′,4′-Tetrahydrospirilloxanthin; (b) *all-trans*-3,4-dihydrorhodovibrin; (c) *all-trans*-3′,4′-dihydroanhydrorhodovibrin.

the other hand, the NOE peaks in ROESY correlate proton pairs that were geometrically close to each other. Thus, the ROESY measurements allow the determination of carotenoid configuration.

Identification of the Component in Peak 4 as 3,4,3′,4′-Tetrahydrospirilloxanthin. Figure 1b shows that peak 4 is the main carotenoid in *R. rubrum* ST4. In FD-MS measurements, peak 4 showed a molecular ion at *m*/*z* 600 (Table 1), suggesting the structure was 3,4,3′,4′-tetrahydrospirilloxanthin. The number of observed signals in the 1D ^{1}H NMR spectrum showed that the carotenoid had a symmetrical structure. The signal at 3.04 ppm was assigned to the protons of both methoxyl groups, and the 1- and 5-methyl protons, and the methylene protons (2-, 3-, 4-H_2) were assigned by the correlation peaks (Table 2a). The olefinic protons within the conjugated chain were assigned on the basis of the splitting patterns and the values of chemical shift in the 1D spectrum and the correlation peaks in the 2D spectra (*38*). Further, the 9- and 13-methyl protons were assigned by the correlation peaks with the olefinic protons. Thus, the NMR data allowed peak 4 to be unambiguously identified as 3,4,3′,4′-tetrahydrospirilloxanthin (1,1′-dimethoxy-1,2,1′,2′-tetrahydro-ψ,ψ-carotene). All the NOE correlation peaks (Figure 2a) established the *all-trans* configuration of the conjugated chain and confirmed our assignment.

Identification of the Component in Peak 2 as 3′,4′-Dihydrorhodovibrin. In FD-MS measurement, peak 2 showed a molecular ion at *m*/*z* 586. The presence of a hydroxyl group was confirmed by FD-MS spectrometry in which the mass of the molecular ion with trimethylsilylation increased by 72 compared to that without trimethylsilylation (Table 1). These results suggested that peak 2 was 3′,4′-dihydrorhodovibrin. The integrated peak area of the signal at 3.04 ppm corresponded to the three protons of a single methoxyl group, and the signals of protons in half of the molecule (2′-H_2 ∼ 15′-H, 1′-Me ∼ 13′-Me) showed the same pattern as those of 3,4,3′,4′-tetrahydrospirilloxanthin. Additionally, the signal at 0.59 ppm had a peak area corresponding to one proton, and could thus be assigned as a hydroxyl group. Although any correlation between the signal assigned to the hydroxyl proton and other protons was not detected in 2D NMR spectra, the presence of a hydroxyl group was confirmed by FD-MS. The 1-methyl H was assigned by the peak area and the value of the chemical shift (1.03 ppm), and the 2-H_2, 3-H_2, and 4-H_2 were assigned by the correlation peaks in the COSY spectrum (Table 2b). All the olefinic protons and the methyl protons within the conjugated chain could be assigned as described in the previous section. Thus, peak 2 was identified unambiguously as 3′,4′-dihydrorhodovibrin (1′-methoxy-1,2,1′,2′-tetrahydro-ψ,ψ-caroten-1-ol). The NOE correlation peaks (Figure 2b) established the *all-trans* configuration of the conjugated chain and confirmed our assignment.

Identification of the Component in Peak 5 as 3,4-Dihydroanhydrorhodovibrin. In FD-MS measurement, peak 5 showed a molecular ion at *m*/*z* 568 (Table 1). This result suggested that peak 5 was 3,4-dihydroanhydrorhodovibrin. The integrated peak area of the signal at 3.04 ppm corresponded to three protons, thus indicating a single methoxy group and the signal of protons at the one side of the molecule (2-H_2 ∼ 15-H, 1-Me ∼ 13-Me) showed the same patterns as those of 3,4,3′,4′-tetrahydrospirilloxanthin. Additionally, the area of the signal at 5.25 ppm corresponded to one proton and was assigned to an olefinic proton (2′-H) at the C2. The end-group was therefore identified as an isopropylidene moiety (ψ end) group. The signals of 3′-H_2 and 4′-H_2 were assigned by the correlation peaks between the 2′-H and both the 3′-H_2 and 4′-H_2 in the COSY spectra (Table 2c). All the olefinic protons and the methyl protons within the conjugated chain were assigned as described in the previous section. Thus, the peak 5 carotenoid was unambiguously identified as 3,4-dihydroanhydrorhodovibrin (1-methoxy-1,2-dihydro-ψ,ψ-carotene). Once again, the NOE correlation peaks (Figure 2c) established the *all-trans* configuration of the conjugated chain and confirmed our assignment.

Identification of the Component in Peak 3 as Rhodopin. The FD-MS spectrum of peak 3 indicated a molecular mass of 554, and the formation of a monotrimethylsilyl derivative indicated the presence of one hydroxyl group. Further, the peak 3 carotenoid should have the same number of conjugated double bonds as the other carotenoids (see Table 1).

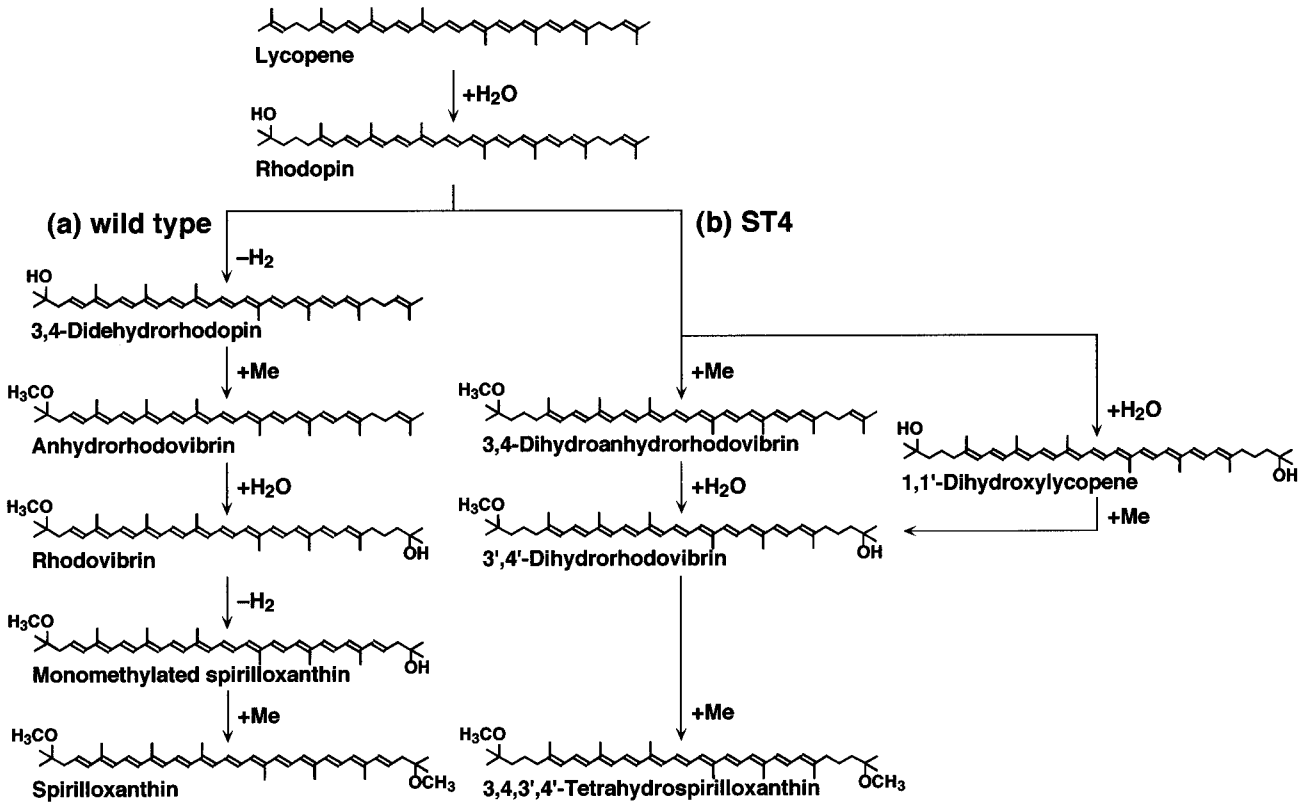

FIGURE 3: Carotenoid biosynthetic pathways in (a) the wild type of *R. rubrum* S1 (see ref *45*) and (b) the proposed variant present in mutant ST4. The precursors found in the mutant have been placed at the same level as their wild-type counterparts.

Therefore, peak 3 was identified as rhodopin (1,2-dihydro-ψ,ψ-caroten-1-ol).

Identification of the Component in Peak 1 as 1,1′-Dihydroxylycopene. Peak 1 was identified by the electronic absorption spectrum and the retention time in HPLC as described below. Peak 1 should have 11 conjugated double bonds (see Table 1). The retention time of peak 1 (Figure 1b) almost corresponded to that of 1,1′-dihydroxylycopene (S. Takaichi, personal communication). We have therefore identified this carotenoid as 1,1′-dihydroxylycopene (1,2,1′,2′-tetrahydro-ψ,ψ-carotene-1,1′-diol). The small amount of material available prohibited further analysis by FD-MS spectrometry and NMR spectroscopy.

We note here that a small amount (0.4% of the total) of lycopene (ψ,ψ-carotene) was also detected by HPLC at 29 min (observable as a very small peak in Figure 1b).

DISCUSSION

A number of studies have shown that the metabolic pathway for the biosynthesis of the carotenoid spirilloxanthin is composed of a linear series of intermediates (Figure 3a). The final product of the pathway, spirilloxanthin, containing 13 conjugated double bonds is incorporated into LH I and RC. It is well-established from classical studies on amino acid auxotrophy (for example, see ref *39*) that the deletion of an enzyme from a linear metabolic pathway usually halts product formation at the deletion locus, and is often accompanied by the accumulation of precursors. This phenomenon is causally related to the stringent substrate specificity of the enzymes involved in the pathway. In this study, it was therefore unexpected that the brown color of a Tn5 deletion mutant arose not from the arrestation of the linear pathway at the level of neurosporene or lycopene but was due principally to 3,4,3′,4′-tetrahydrospirilloxanthin, which lacks a conjugated double bond at each end of the symmetrical molecule.

The lack of conjugated double bonds at both the 3,4- and 3′,4′-positions of the symmetrical molecule strongly suggests that the Tn5 lesion is present in the gene for rhodopin 3,4-desaturase, and that this enzyme may be responsible for dehydrogenation at both ends of the molecule. Thus, in the absence of rhodopin 3,4-desaturase, two new intermediates, 3,4-dihydroanhydrorhodovibrin and 3′,4′-dihydrorhodovibrin, would be predicted if the specificity of the following enzymes would be broad enough to accept a carotenoid substrate with only 11 conjugated double bonds (Figure 3). It is therefore satisfying that the putative intermediates of this branched pathway could also be determined in this study. Finally, the observation of a fourth novel carotenoid, 1,1′-dihydroxylycopene, in the mutant suggests that even the order of methylation or hydroxylation of the end groups is not obligatory. We therefore conclude that the pathway of spirilloxanthin biosynthesis in *R. rubrum* has inherent capacity for branching, where in principle the order of (at least) rhodopin modification can occur randomly. That this is not observed in the wild-type organism is probably due to a kinetic "matching" of enzymatic steps, which probably becomes imbalanced when an enzyme of the pathway is deleted. However, two studies have primarily indicated that 3,4-dihydrospirilloxanthin is present as a minor (approximately 10% of the total) carotenoid in wild-type cultures of *R. rubrum* S1 (*23*, *36*). The broad substrate specificity of the later carotenoid biosynthesis enzymes would explain the until now puzzling observation (*22*, *24*−*26*) that the addition

of the inhibitor DPA to growing cultures of *R. rubrum* causes the production of a large number of nonnatural carotenoids. Our data suggest that the DPA effect is probably due to differential inhibition of the various enzymes of the carotenoid pathway, including the 3,4-desaturase, thus causing an ill-defined combinational branching. In this context, it has also been shown recently by Takaichi et al. (*40*) that the lycopene cyclase of *Erwinia uredovora* also shows a broader substrate specificity than had previously been supposed.

Branching of the carotenoid biosynthesis pathway in the phototrophic bacteria *Rb. capsulatus* and *Rb. sphaeroides* has been shown to occur naturally. In these organisms, the order of end-group modification of the precursor hydroxyneurosporene occurs by the sequential but random action of the *crtD* and *crtF* gene products, to form spheroidene (*3*, *12*, *15*). In addition, the *crtC* and *crtA* gene products also have a dual function, acting on neurosporene and spheroidene, and spheroidene and hydroxyspheroidene, respectively (*3*, *12*, *15*). Finally, neurosporene is formed from phytoene by the sequential action of the *crtI* gene product, phytoene desaturase. This low substrate specificity of the *crtI* gene is common to most organisms examined so far (see ref *2*). Taken together with the present data, we conclude that the intrinsically broad substrate specificity of the enzymes of carotenoid biosynthesis may be retained even in organisms exhibiting apparently linear pathways.

Southern hybridization experiments have shown that only a single Tn5 lesion is present in the chromosome of *R. rubrum* ST4 (data not shown). In addition, the successful complementation of the mutant with a 20 kb fragment from wild-type *R. rubrum* suggests that the Tn5 lesion is responsible for the observed phenotype. However, as we have not yet mapped the *crt* operon(s) encoding the genes for carotenoid biosynthesis completely, we cannot yet exclude the possibility that the transcription of more than a single gene has been interrupted by the Tn5 element. Nevertheless, the observation of the expected intermediate carotenoids predicted for a single gene lesion is strong evidence that only a single gene has been affected. We have mapped this gene [previously designated *crtX* (*27*), see also ref *41* for a comparison with the *psg* clusters from other phototrophic bacteria] to the *psg* superoperon of *R. rubrum*, and the organization of the *crt* operon(s) therein is presently being examined. Our interpretation of the Tn5 lesion would imply that the *crt* operon is organized differently than those of *Rb. capsulatus* (*3*, *15*) and *Rb. sphaeroides* (*12*), where the corresponding functional gene, *crtD*, is the first of a *crtD-crtC* cistron.

Finally, although we have not isolated LH I or RC complexes in this study, the position of the bacteriochlorophyll Q_y absorption band of the LH I complexes from *R. rubrum* ST4 at 882 nm is characteristic of the presence of bound carotenoid and identical to that of wild-type complexes. It is now well-established that in the absence of carotenoid the 882 nm absorption maximum is blue-shifted to 873−875 nm (*42*). We therefore conclude that the LH I complexes are able to bind the nonnatural carotenoid 3,4,3′,4′-tetrahydrospirilloxanthin. In this study, we cannot yet ascertain as to whether the other three new carotenoids are bound by the photosynthetic complexes. However, for wild-type cells, there is good evidence that *all* of the intermediates proceeding from phytoene are incorporated into the photosynthetic complexes during growth and that carotenoid maturation proceeds *in situ* (*23*, *43*), although an exchange of LH I-bound carotenoids with a biosynthetic pool cannot yet be excluded. In addition, the cells are able to grow normally under both anaerobic, photoheterotrophic conditions as well as aerobic, chemoheterotrophic conditions, indicating no toxicity due to carotenoid accumulation. In *Rb. sphaeroides*, the LH I complexes also appear to have a broad substrate binding specificity, as heterologously expressed carotenoids from *Erwinia herbicola* can also be incorporated (*44*).

In summary, the mutant *R. rubrum* ST4 appears to present an unusual and interesting model system for investigating the roles of carotenoids in bacterial photosynthetic complexes. In particular, we expect the biophysics of light harvesting and energy transfer for complexes containing only 11 double bonds but otherwise identical to those of wild-type to be of great interest. In addition, the present study indicates that the organization of the *crt* operon(s) in *R. rubrum* may be unusual. Both of these aspects are under investigation by our groups at the present time.

ACKNOWLEDGMENT

We thank R. J. Strasser (Laboratory of Bioenergetics, University of Geneva) for encouragement and support during the course of this work. We also thank M. F. Blanc for expert technical assistance.

REFERENCES

1. Krinsky, N. I. (1993) *Annu. Rev. Nutr. 13*, 561−587.
2. Armstrong, G. A., Alberti, M., and Hearst, J. E. (1990) *Proc. Natl. Acad. Sci. U.S.A. 87*, 9975−9979.
3. Armstrong, G. A., Schmidt, A., Sandmann, G., and Hearst, J. E. (1990) *J. Biol. Chem. 265*, 8329−8338.
4. Armstrong, G. A., Cook, D. N., Ma, D., Alberti, M., Burke, D. H., and Hearst, J. E. (1993) *J. Gen. Microbiol. 139*, 897−906.
5. Armstrong, G. A., Hundle, B. S., and Hearst, J. E. (1993) *Methods Enzymol. 214*, 297−311.
6. Armstrong, G. A. (1995) in *Anoxygenic Photosynthetic Bacteria* (Blankenship, R. E., Madigan, M. T., and Bauer, C. E., Eds.) pp 1135−1157, Kluwer Academic Publishers, Dordrecht.
7. Bartley, G. E., Schmidhauser, T. J., Yanofsky, C., and Scolnik, P. A. (1990) *J. Biol. Chem. 265*, 16020−16024.
8. Bartley, G. E., and Scolnik, P. A. (1995) *Plant Cell 7*, 1027−l038.
9. Sandmann, G. (1991) *Physiol. Plant. 83*, 186−193.
10. Bramley, P. M., and MacKenzie, A. (1988) *Curr. Top. Cell. Regul. 29*, 291−343.
11. Armstrong, G. A. (1994) *J. Bacteriol. 176*, 4795−4802.
12. Lang, H. P., Cogdell, R. J., Takaichi, S., and Hunter, C. N. (1995) *J. Bacteriol. 177*, 2064−2073.
13. Sandmann, G. (1994) *Eur. J. Biochem. 223*, 7−24.
14. Giuliano, G., Pollock, D., and Scholnik, P. A. (1986) *J. Biol. Chem. 261*, 12925−12929.
15. Armstrong, G. A., Alberti, M., Leach, F., and Hearst, J. E. (1989) *Mol. Gen. Genet. 216*, 254−268.
16. Gari, E., Toledo, J. C., Gibert, I., and Barbe, J. (1992) *FEMS Microbiol. Lett. 93*, 103−108.
17. McGlynn, P., and Hunter, C. N. (1993) *Mol. Gen. Genet. 236*, 227−234.
18. Misawa, N., Nakagawa, M., Kobayashi, K., Yamano, S., Izawa, Y., Nakamura, K., and Harashima, K. (1990) *J. Bacteriol. 172*, 6704−6712.
19. Hundle, B. S., Beyer, P., Kleinig, H., Englert, G., and Hearst, J. E. (1991) *Photochem. Photobiol. 54*, 89−93.

20. Liaaen-Jensen, S., Cohen-Bazire, G., Nakayama, T. O. M., and Stanier, R. Y. (1958) *Biochim. Biophys. Acta 29*, 477−498.
21. Liaaen-Jensen, S., Cohen-Bazire, G. and Stanier, R. Y. (1961) *Nature 192*, 1168−1172.
22. Davies, B. H., and Than, A. (1974) *Phytochemistry 13*, 209−219.
23. Naruse, M., Hashimoto, H., Kuki, M., and Koyama, Y. (1991) *J. Mol. Struct. 242*, 15−26.
24. Davies, B. H. (1970) *Biochem. J. 116*, 101−110.
25. Malhotra, H. C., Britton, G., and Goodwin, T. W. (1970) *Phytochemistry 9*, 2369−2375.
26. Malhotra, H. C., Britton, G., and Goodwin, T. W. (1970) *FEBS Lett. 6*, 334−336.
27. Saegesser, R. (1992) Ph.D thesis, University of Zurich.
28. Sistrom, W. R. (1960) *J. Gen. Microbiol. 22*, 778−785.
29. Regensburger, B., Meyer, L., Filset, M., Weber, J., Studer, D., Lamb, J. W., Fischer, H.-M., Hahn, M., and Hennecke, H. (1986) *Arch. Microbiol. 144*, 355−366.
30. Ghosh, R., Elder, D. J. E., Saegesser, R., Kelly, D. J., and Bachofen, R. (1994) *Gene 150*, 97−100.
31. Ghosh, R., Hardmeyer, A., Thoenen, I., and Bachofen, R. (1994) *Appl. Environ. Microbiol. 60*, 1698−1700.
32. Connor, A. E., and Britton, G. (1990) in *Current Research in Photosynthesis* (Baltscheffsky, M., Ed.) Vol. 2, pp 53−56, Kluwer Academic Publishers, Dordrecht.
33. Jiang, Y.-S., Kurimoto, Y., Shimamura, T., Ko-chi, N., Ohashi, N., Mukai, Y., and Koyama, Y. (1996) *Biospectroscopy 2*, 47−58.
34. Takaichi, S. (1993) *Org. Mass Spectrom. 28*, 785−788.
35. Britton, G. (1995) in *Carotenoids* (Britton, G., Liaaen-Jensen, S., and Pfander, H., Eds.) Vol. 1B, pp 13−62, Birkhäuser Verlag, Basel.
36. Koyama, Y., Takatsuka, I., Kanaji, M., Tomimoto, K., Kito, M., Shimamura, T., Yamashita, J., Saiki, K., and Tsukida, K. (1990) *Photochem. Photobiol. 51*, 119−128.
37. Takaichi, S., and Shimada, K. (1992) *Methods Enzymol. 213*, 374−385.
38. Koyama, Y., Kanaji, M., and Simamura, T. (1988) *Photochem. Photobiol. 48*, 107−114.
39. Bonner, D., Tatum, E. L., and Beadle, G. W. (1943) *Arch. Biochem. 3*, 71−91.
40. Takaichi, S., Sandmann, G., Schnurr, G., Satomi, Y., Suzuki, A., and Misawa, N. (1996) *Eur. J. Biochem. 241*, 291−296.
41. Bauer, C. E., Bollivar, D. W., and Suzuki, J. Y. (1993) *J. Bacteriol. 175*, 3919−3925.
42. Wiggli, M., Cornacchia, L., Saegesser, R., Bachofen, R., and Ghosh, R. (1996) *Microbiol. Res. 151*, 57−62.
43. Schwerzmann, R. U., and Bachofen, R. (1989) *Plant Cell Physiol. 30*, 497−504.
44. Hunter, C. N., Hundle, B. S., Hearst, J. E., Lang, H. P., Gardiner, A. T., Takaichi, S., and Cogdell, R. J. (1994) *J. Bacteriol. 176*, 3692−3697.
45. Schmidt, K. (1978) in *The Photosynthetic Bacteria* (Clayton, R. K., and Sistrom, W. R., Eds.) pp 729−750, Plenum Press, New York.

BI9730947